Bone Reports 13 (2020) 100707

Contents lists available at ScienceDirect

Bone Reports

journal homepage: www.elsevier.com/locate/bonr

Effect of long term palmitate treatment on osteogenic differentiation of human mesenchymal stromal cells - Impact of albumin

Kristina Glenske[a,*,1], Kaija Schäpe[b,1], Anneke Wieck[c], Klaus Failing[d], Janina Werner[a], Marcus Rohnke[b], Sabine Wenisch[a,1], Sybille Mazurek[c,1]

[a] Clinic of Small Animals, c/o Institute of Veterinary Anatomy, Histology and Embryology, Justus-Liebig-University of Giessen, Giessen, Germany
[b] Institute of Physical Chemistry, Justus-Liebig-University of Giessen, Giessen, Germany
[c] Institute of Veterinary Physiology and Biochemistry, Justus-Liebig-University of Giessen, Giessen, Germany
[d] Unit for Biomathematics and Data Processing, Faculty of Veterinary Medicine, Justus-Liebig-University of Giessen, Giessen, Germany

ARTICLE INFO

Keywords:
Human mesenchymal stromal cells
BSA
Osteogenic marker genes
ToF-SIMS
Glycolysis
Glutaminolysis

ABSTRACT

The long-term effects of palmitate (PA) on osteogenic differentiation capacity of human mesenchymal stromal cells (hMSCs) were investigated by cultivating the cells in osteogenic differentiation medium (O-w/o) and osteogenic medium containing PA (O-BSA-PA) for 21 days. Osteogenic medium containing BSA (O-BSA) was used as a control. By means of rt-qPCR, successful osteogenic differentiation was observed in the O-w/o regarding the levels of osteogenic and cell-communication related genes (*OCN*, *Col1*, *BMP2*, *ITGA1*, *ITGB1*, *Cx43*, *sp1*) in contrast to expression levels observed in cells incubated within basal medium. However, in the O-BSA, these genes were found to have decreased significantly. In cases of *Cx43* and *sp1*, PA significantly reinforced the reductive effect of BSA alone. O-BSA notably decreased glucose and pyruvate consumption, whereas glutamine consumption significantly increased. In comparison to O-BSA addition of PA significantly reduced glycolysis and glutaminolysis. ToF-SIMS analysis confirmed increased incorporation of supplemented deuterated PA into the cell membranes, while the overall PA-concentration remained unchanged compared to cells incubated in the O-BSA and O-w/o. Therefore, the effects on gene expression and the metabolism did not result from the membrane alterations, but may have risen from inter- and intracellular effects brought on by BSA and PA.

1. Introduction

Both osteoblasts and bone marrow adipocytes derive from mesenchymal stromal cells (MSCs). Due to their common progenitor cell, a reciprocal relationship between osteoblastogenesis and adipogenesis has been assumed (Chen et al., 2016; Clabaut et al., 2010; Muruganandan et al., 2009). During aging and in the course of osteoporosis, a substantial increase in bone marrow adipocytes is observed (Meunier et al., 1971; Singh et al., 2016; Verma, 2002). The bone marrow adipocytes, attained from osteoporotic patients, are characterized by an increased content of palmitate, as well as an increased ratio of saturated vs. unsaturated fatty acids (Pino et al., 2016). Fatty acid analysis of bone marrow supernatant fluids from postmenopausal women reveals a dynamic fatty acid composition which is notably different from that of the blood plasma. This finding has led to the assumption that lipids have localized impacts on cellular differentiation (Miranda et al., 2016). In a previous study, we have shown that palmitate content of the cell membrane (FA(16:0)) decreases during osteogenic differentiation of hMSCs isolated from a non-osteoporotic donor (Schaepe et al., 2017). Although there are numerous studies dealing with the impact of different fatty acids on osteoblastogenesis in primary human (Elbaz et al., 2010; Gunaratnam et al., 2013; Kim et al., 2008; Maurin et al., 2002) and rat (Yeh et al., 2013; Yeh et al., 2014) osteoblasts, the exact impact of fatty acids on osteogenic differentiation is still unclear. While a number of studies (Gunaratnam et al., 2013; Kim et al., 2008; Lucas et al., 2013; Wang et al., 2013) indicate an inhibition of cell proliferation and differentiation, as well as an induction of apoptosis by palmitate, others (Yeh et al., 2014) were not able to provide evidence for the influence of palmitate on these functions. Indirect co-culture studies with osteoblasts and fatty acid producing adipocytes, as well as the usage of an adipocyte-conditioned medium (from adipocyte monocultures) in osteoblast-monocultures, reveals that adipocytes are able to induce adipogenic differentiation of osteoblasts (Clabaut et al., 2010) and to reduce osteoblast functioning

* Corresponding author.
E-mail address: Kristina.Glenske@vetmed.uni-giessen.de (K. Glenske).
[1] Authors contributed equally.

https://doi.org/10.1016/j.bonr.2020.100707
Received 28 January 2020; Received in revised form 22 July 2020; Accepted 30 July 2020
Available online 13 August 2020

(Wang et al., 2013). An adverse effect on osteoblasts was also observed when palmitate and stearate were supplemented to osteoblast monocultures by means of the conditioned medium (Elbaz et al., 2010; Wang et al., 2013). Direct palmitate supplementation into cell culture media is shown to induce concentration- and time dependent apoptosis in different cell species, including mature osteoblasts (Gunaratnam et al., 2013; Hickson-Bick et al., 2002; Kim et al., 2008). Palmitate-induced apoptosis of osteoblasts is circumvented by co-supplementation of the adenosine monophosphate kinase (AMPK) activator (AICAR), which triggers the extracellular signal-regulated kinases (ERK) signalling pathway (Kim et al., 2008). AMPK is an important sensor of energy deficiency, which activates energy producing metabolic pathways i.e. fatty acid and glucose degradation. On the other hand AMPK inhibits synthetic processes such as fatty acid synthesis and glycogen synthesis, thereby regulating the homeostasis between energy regenerating and energy consuming metabolic processes.

In co-cultures of osteoblasts and differentiating pre-adipocytes, the negative impact of fatty acids, such as palmitate biosynthesized from the adipocytes, could be circumvented by an inhibition of acetyl CoA carboxylase and fatty acid synthase in the adipocytes (Elbaz et al., 2010), stimulation of the palmitate degradation (Yeh et al., 2014), as well as specific inhibitors of autophagy or apoptosis (Gunaratnam et al., 2013). All co-cultivation studies, and studies investigating the impact of palmitate on adipogenesis and osteogenesis as mentioned above, are based on cultivation and incubation times respectively between 20 and 72 h (Clabaut et al., 2010; Gunaratnam et al., 2013; Hickson-Bick et al., 2002; Kim et al., 2008; Lucas et al., 2013; Maurin et al., 2002; Wang et al., 2013; Yeh et al., 2014, 2014). In summary, these studies suggest a reduction of osteoblast function during short-term incubation of the cell cultures by palmitate.

In the present study we investigated the impact of long-term (21 days) constant palmitate supplementation on osteogenic differentiation of human MSCs in order to simulate chronic exposure. The impact of palmitate on the differentiation capacity of hMSCs was characterized by determining gene expression of different osteoblast marker genes (Wang et al., 2015). In detail, an analysis of *Runx2* was conducted as an early marker of osteogenic differentiation, and the late markers bone morphogenetic protein 2 (*BMP2*), collagen 1 (*col1*), and osteocalcin (*OCN*). Integrin α5 (*ITGA5*), integrin β1 (*ITGB1*), connexin43 (*Cx43*) and its transcription factor sp1 (*sp1*) were investigated. Since several studies reveal a shift from glycolytic to mitochondrial energy production during osteogenic differentiation (Chen et al., 2008; Pattappa et al., 2011), the impact of palmitate on the conversion rates of key metabolic substrates and products in the medium supernatants of the cells was measured. In order to investigate whether palmitate, supplemented into the cultivation medium of the cells, changes the fatty acid composition of the membrane, we analysed the palmitate content of the hMSCs cell membranes using time-of-flight secondary ion mass spectrometry (ToF-SIMS) (Gulin et al., 2017; Johansson, 2006; Schaepe et al., 2017).

Palmitate itself is not soluble in cell culture media unless complexed with albumin. In serum, its association with albumin plays an active role in the cellular uptake of long chain fatty acids (Abumrad et al., 2000; Trigatti and Gerber, 1995). Accordingly, palmitate was supplemented to the media in combination with bovine serum albumin (BSA) and the impact of BSA was taken into account in the experimental design.

2. Material and methods

2.1. Isolation and cultivation of primary bone-derived hMSCs

The human bone-derived mesenchymal stromal cells were isolated from femoral heads in accordance with a previously published protocol (Glenske et al., 2019; Schaepe et al., 2017; Wagner et al., 2017; Wenisch et al., 2005; Wenisch et al., 2006). The femoral heads of three female patients, who had undergone total hip arthroplasty, were provided by Asklepios Clinic Lich GmbH (Lich, Germany). The experiments were approved by the local ethics committee of the Medical Faculty of the Justus Liebig University Giessen (decisions 05/06 and 106/06).

The femoral heads were sawn into small discs and the compacta was detached. The spongiosa pieces were cultured in a petri dish with standard medium, consisting of α-MEM (minimum essential medium) (Life Technologies – Thermo Fisher Scientific, Darmstadt, Germany), 20% (*v*/v) FBS (Biochrome, Berlin, Germany) and 100 U/ml penicillin/streptomycin (PAA Laboratories, Pasching, Austria) at humidified atmosphere (5% CO_2, 37 °C). The human mesenchymal stromal cells (hMSCs) distanced themselves from the bone and adhered to the petri dishes. After 1–2 weeks, the bone pieces were removed and the cells were cultured in a medium which was replaced twice a week. Passaging took place when reaching 80% confluence. For experiments, cells of the three donors in the fourth passage were pooled.

The hMSCs were seeded with 20,000 cells per well (1.9 cm^2) in tissue culture plates for RNA-extraction and metabolome analyses. For the analysis using ToF-SIMS, hMSCs were cultured on silicon wafers (5000 cells at 1 cm^2) which were cleaned with demineralized water, acetone and 70% ethanol beforehand, according to a previously published protocol (Schaepe et al., 2015).

2.2. Preparation of fatty acid BSA stock solution

Briefly, 2 mM palmitate (PA; Cat.-No 489662-1G, Sigma-Aldrich, Steinheim, Germany) in 0.15 mM sodium chloride solution (NaCl, Carl Roth GmbH, Karlsruhe, Germany) was incubated at 70 °C for 60 min. Simultaneously, 0.45 mM fatty acid-free BSA (FFA-BSA; Cat.-No A8806-1G, Sigma-Aldrich, Missouri, USA) was incubated at 37 °C, for 60 min, in 0.15 mM sodium chloride and filter sterilized. The palmitate and BSA solutions were mixed 1:2 and incubated at 37 °C, for 60 min, leading to a molar ratio of palmitate:BSA of 4.4:1. For the ToF-SIMS experiments, deuterated palmitate (dPA; Cat.-No P0500-10G, Sigma-Aldrich, Steinheim, Germany) was used. The stock solutions were supplemented into the cultivation media in final concentrations of 0.045 mM BSA and 0.2 mM PA.

2.3. Osteogenic differentiation in the presence and absence of BSA and BSA + PA, respectively

Twenty-four hours after passaging, the standard medium was changed to osteogenic differentiation medium (OM), which consisted of α-MEM supplemented with 10% (v/v) FBS, 100 U/ml penicillin/streptomycin, 10 mM β-glycerophosphate, 0.06 mM ascorbic acid and 0.1 μM dexamethasone (all Sigma-Aldrich, Steinheim, Germany) (Glenske et al., 2019; Wagner et al., 2017; Wenisch et al., 2005). As controls hMSCs were cultured in basal medium (BM) without osteogenic supplements (α-MEM with 10% (v/v) FBS and 100 U/ml penicillin/streptomycin). Depending upon the experiment, both cultivation media (OM and BM) were supplemented with 0.2 mM BSA-PA (palmitic-acid dissolved in bovine serum albumin as described above) or 0.045 mM BSA alone. The cultivation was conducted for 21 days in all six approaches (BM-w/o, BM-BSA, BM-BSA-PA, OM-w/o, OM-BSA, OM-BSA-PA) and the media were replaced twice a week.

2.4. Real-time quantitative polymerase chain reaction (rt-qPCR)

The analysis of gene expression in the cells cultivated for 21 days, in all six media (with four replicates per medium), was performed by means of rt-qPCR. The RNA-extraction was performed with the innuPREP RNA Mini Kit (Analytic Jena AG, Jena, Germany) according to the manufacturer's protocol. Extracted RNA was stored in liquid nitrogen.

The transcription of cDNA was carried out in accordance with a previously published protocol (Glenske et al., 2014). The rt-qPCR was

carried out in triplets with the Qiagen Quanti Fast SYBR Green PCR Kit (Qiagen, Hilden, Germany) combined with QuantiTect Primer Assays (Qiagen, Hilden, Germany) as described previously (Glenske et al., 2014).

In this study, the following QuantiTect Primer Assays were used: bone morphogenetic protein 2 (*BMP-2*, Qiagen-ID: QT00012544), collagen I (*Col1*, Qiagen-ID: QT00037793), connexin 43 (*Cx43*, Qiagen-ID: QT00012684), integrin alpha 5 (*ITGA5*, Qiagen-ID: QT00080871), integrin beta 1 (*ITGB1*, Qiagen-ID: QT00068124), osteocalcin (*OCN*, Qiagen-ID: QT00232771), runt-related transcription factor 2 (*Runx2*, Qiagen-ID: QT00020517), and sp1 transcription factor (*sp1*, Qiagen-ID: QT01870449). The expression of glyceraldehyde-3 phosphate dehydrogenase (*GAPDH*, Qiagen-ID: QT00079247) was not influenced by BSA and BSA-PA-treatment and was, therefore, used as a housekeeping gene.

The data was analysed using the ΔΔCt-method for gene expression with the corresponding basal gene expressions (BM-w/o, BM-BSA, BM-BSA-PA) as control.

2.5. Metabolic conversion rates

On the 21st cultivation day, the respective cultivation supernatants (O-w/o, O-BSA, O-BSA-PA) were renewed one last time. After 48 h, the cultivation supernatants of the finally differentiated cells (six wells per medium) were collected, centrifuged at 200 ×*g* for 4 min and frozen immediately at −80 °C. In order to determine the turnover rates of the respective metabolites in the 48-hour incubation period, plates with the same media additives (O-w/o, O-BSA, O-BSA-PA) but without cells were cultivated parallel to the individual batches containing cells. The cells in the corresponding wells (6 replicates per medium) were washed three times with phosphate buffered saline (PBS) and frozen at −80 °C for 30 min. For protein determination, the frozen wells were incubated with RIPA-buffer for 30 min. The cells were then removed from the dishes and centrifuged at 12,000 ×*g* for 20 min. In the supernatants the protein content was analysed using the BCA-assay, as described by Wu et al. (Wu et al., 2015).

In order to determine the metabolic conversion rates of the cells, the frozen medium supernatants from dishes with cells as well as dishes without cells were heated to 95 °C for 10 min. Thereafter, they were centrifuged at 16,000 ×*g* for a further 10 min in order to inactivate enzyme activities, within the medium samples, which derived from FBS. Glucose, lactate, pyruvate, glutamine, glutamate and serine were determined photometrically using a benchtop random clinical analyser, as described by Unterluggauer et al. (Unterluggauer et al., 2008). The extraction efficiencies were 95% for glucose, 99% for lactate, 118% for pyruvate, 121% for serine, 95% for glutamate and 82% for glutamine (calculated from mean values of 5 experiments). Standard solutions of all metabolites were run simultaneously to the samples in order to confirm the accuracy of the measurements. The conversion rates of the different metabolites were calculated as the difference between the metabolite concentrations in medium samples from dishes containing cells and medium samples from dishes cultivated without cells on the same days. The calculation was performed according to the following formula: metabolite conversion in [nmol/(h * µg protein)] = metabolite concentration [nmol/dish] in medium containing cells at t_{48} minus metabolite concentration [nmol/dish] in medium without cells at t_{48} divided by (48 h * µg protein).

2.6. Chemical fixation for ToF-SIMS analysis

In order to introduce the cells into the ultra-high vacuum system for ToF-SIMS analysis, the cells cultivated in the three osteogenic media (OM-w/o, OM-BSA, OM-BSA-PA, with 4 replicates per medium) were chemically fixed with a 3% fixative containing 2% paraformaldehyde (PFA) (Carl Roth GmbH, Karlsruhe, Germany) and 1% glutaraldehyde (Agar Scientific Ltd., Essex, UK). Thereafter, they were washed and stored in Milli-Q water until analysis continued. Previously we have shown that this preparation and water-storage is optimal when aiming to preserve and study the plasma membrane fatty acid composition (Schaepe et al., 2015; Schaepe et al., 2016).

2.7. Time-of-flight secondary ion mass spectrometry

A TOF.SIMS 5 instrument (ION-TOF, Münster, Germany) equipped with a pulsed bismuth primary ion source (25 keV) was employed for data acquisition.

For the assessment of relative concentration changes, the instrument was operated in spectrometry mode (also called high-current bunched mode). This mode features a high reproducibility and the instrument's highest achievable mass resolution with a spatial resolution below 10 µm. Mass resolution (FWHM) was $R > 5500$ at m/z 78.96 (PO_3^-) for negative ion mode. To image the incorporation of palmitate in the cells' plasma membrane, the so-called fast imaging (or non-bunched burst alignment) mode, combined with delayed extraction, was employed. This led to a comparable mass resolution ($R > 5000$ at m/z 78.96 (PO_3^-)) with an improved spatial resolution below 500 nm (Vanbellingen et al., 2015). Bi_3^+ clusters were applied as primary ions on an analysis area of 150 × 150 µm^2. In spectrometry mode, a primary ion current of 0.5–0.08 pA was rastered in sawtooth mode and with 128 × 128 pixels, at one shot per pixel, until a comparable total ion dose of 1×10^{12} ions/cm^2 was reached in all measurements. In fast imaging mode, 20 scans with random rastering at 512 × 512 pixels and three shots per pixel were compared, while an extraction delay of 0.240 µs was set. For data evaluation, the software Surfacelab 6.7 was employed (ION-TOF). Negative mode signals CH^-, CH_2^-, OH^-, C_2H^-, C_4H^-, PO_2^-, PO_3^-, $C_{18}H_{35}O_2^-$ were used.

2.8. Statistical analyses

Statistics of the gene expression profiles were obtained by one-way ANOVA and Tukey's multiple comparison test in GraphPad Prism (GraphPad Software, Inc.).

Statistical analysis of the metabolome measurements was performed using the software package BMDP (Dixon 1993). After one-way ANOVA, a subsequent Dunnett test was conducted in order to compare O-w/o and O-BSA-PA with O-BSA control group. In all cases, the level of significance was set at $p \leq 0.05$.

Statistics of the relevant palmitate signals, normalized to the PO_3^- signal, were analysed using one-way ANOVA and Tukey's multiple comparison test in GraphPad Prism (GraphPad Software, Inc.).

3. Results and discussion

3.1. Gene expression on mRNA-level

By means of rt-qPCR, the expression patterns of osteogenic markers were investigated in order to analyse the degree of osteogenic differentiation of the hMSCs as well as the level of cell-matrix-, and cell-cell-communication of the cultures, due to the BSA and palmitate (PA) supplementation of the media (O-BSA and O-BSA-PA). The interaction between the markers investigated presently (*BMP2*, *Col1*, *OCN*, *Runx2*, *Cx43*, *sp1*, *ITGA5* and *ITGB1*) is shown in Fig. 1.

3.1.1. Osteogenic differentiation

After 21 days of cultivation in the osteogenic differentiation medium without supplements (O-w/o), the gene expression of the hMSCs revealed an increase in *Runx2* (3.8 fold-change), *BMP2* (8.5 fold-change), *OCN* (3.1 fold-change) and *Col1* (3.4 fold-change) in comparison to the corresponding basal cultivation approach (B-w/o), which was used as a control for normalization (Fig. 2). Increased expression of these genes indicated a successful osteogenic differentiation of hMSCs (Glenske et al., 2019). Runt-related transcription factor 2 (*Runx2*) is

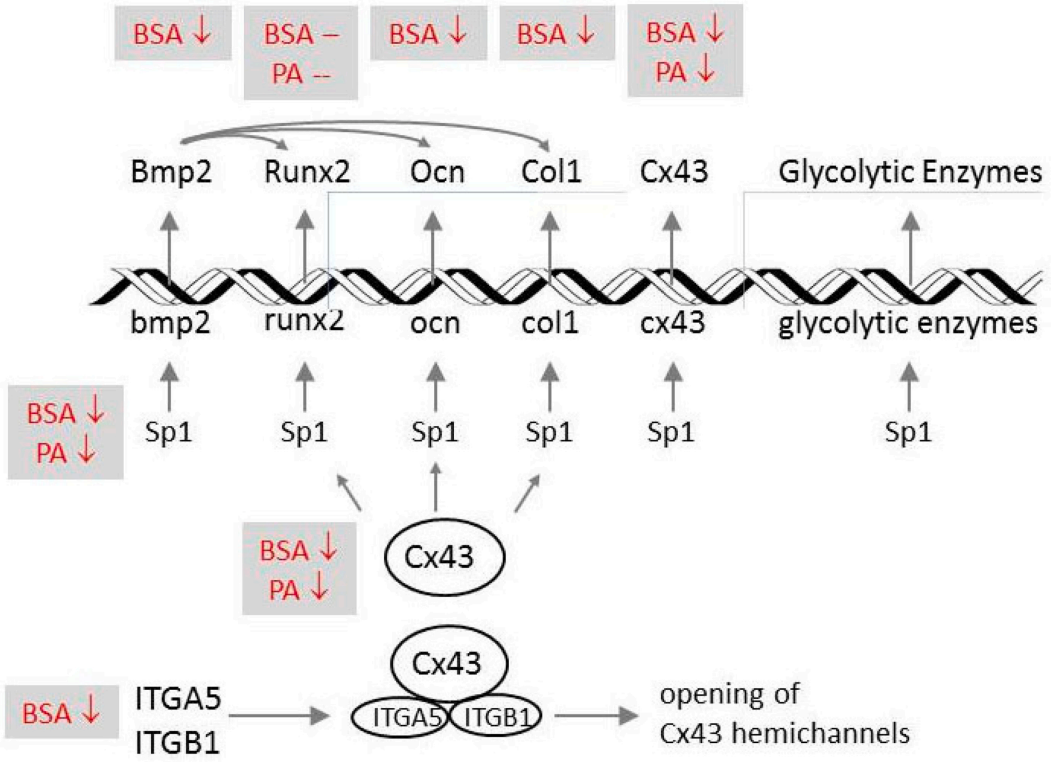

Fig. 1. Interaction between BMP2, Col1, OCN, Runx2, Cx43, sp1, ITGA5, ITGB1 and glycolytic enzyme expression.
Transcription factor Sp1 activates the expression of *BMP2*, *Runx2*, *Col1*, *OCN*, *Cx43* as well as several glycolytic enzymes. BMP2 may induce the expression of *Runx2*, *OCN* and *Col1*. Cx43 activates the binding of Sp1 to the promotors of *Runx2*, *Col1* and *OCN*. BSA leads to a decrease in the expression of *BMP2*, *OCN*, *Col1*, *ITGA5* and *ITGB1*, *Cx43* and *Sp1* when compared to hMSCs osteogenic differentiated in the absence of BSA. For PA a significant attenuation was only detectable for *Cx43* and *sp1* expression when compared to BSA-treated hMSCs.

expressed in osteoblasts during the early phase of osteogenic differentiation (Long, 2011). Runx2 expression is necessary for the activation of osteoblast marker genes, such as osteocalcin (*OCN*) and collagen I (*Col1*) (Vimalraj et al., 2015). Collagen 1 is synthesized by osteoblasts as a major component of the extracellular matrix (ECM) (Long, 2011) and its gene expression increases in a time-dependent pattern during osteogenic differentiation (Wang et al., 2015). In hMSCs of osteoporotic donors, *Col1* expression is reduced and associated with poor osteogenic capability of the cells (Pino et al., 2012).

Bone morphogenetic protein 2 (BMP2) promotes osteogenic differentiation in vivo and in vitro (Katagiri and Takahashi, 2002; Sun et al., 2015). BMPs are characterized by their ability to induce ectopic bone formation (Katagiri and Takahashi, 2002). BMP2 induces subsequent osteogenic differentiation of rat bone MSCs (Sun et al., 2015) and skeletal myoblasts (mice) (Gersbach et al., 2007). This is accompanied by an increase of *OCN*, *Col1* and *Runx2* gene expression, which is associated with increased mineralization and adhesion strength of the cells (Sun et al., 2015).

Osteocalcin (OCN) is the most frequently occurring non-collagenous extracellular matrix (ECM)-protein synthesized by osteoblasts (Ducy et al., 1996; Katagiri and Takahashi, 2002) and has been reported as an osteoblast specific hormone (Wei and Karsenty, 2015). Circulating osteocalcin (in human blood) can be used as a specific marker for bone-turnover (Polak-Jonkisz and Zwolinska, 1998).

In the present study, *Runx2* expression of the cells cultured in all the osteogenic differentation approaches (O-w/o, O-BSA and O-BSA-PA) was four fold-change higher in comparison to cells cultivated in the corresponding basal medium used for normalization (Fig. 2). The increased levels of *Runx2* expression suggested a successful induction of the osteogenic differentiation in all osteogenic media irrespective of the addition of BSA or BSA-PA (Fig. 2). Gunaratnam et al. (Gunaratnam et al., 2014) describe a significant decrease in *Runx2* and *OCN* during osteogenic differentation of human osteoblasts from day one to day seven of PA-treatment (2.5 mM BSA + 250 μM PA) (Gunaratnam et al., 2014). The PA concentrations used by Gunaratnam et al. were similar to the presently used PA concentrations, whereas the BSA concentrations (2.5 mM) were higher than the concentration used in our approach (supplemented with 0.045 mM). Nevertheless, a methodological concern is the FBS containing albumin and lipid species used for medium preparation, however this is a constant throughout the experiment.

Whereas *Runx2* expression of the cells did not differ significantly between the three osteogenic differentiation media, *BMP2* and *Col1* significantly decreased in the BSA treated group (O-BSA) compared to the O-w/o-cells.

In summary, the expression patterns of the osteogenic markers *Runx2*, *BMP2*, *OCN*, *Col1* (Fig. 2) suggested significant effects of suppression of BSA long-term treatment (21 days) on the osteogenic differentiation capacity of hMSCs. Concomitant treatment of these cultures with BSA and PA led to no significant changes in gene expression. In contrast to our findings, it has been shown by Yeh et al., that short-term treatment (48 h) of fetal rat calvarial cells with 100 μM PA, leads to reduced bone nodule formation and decreased RNA-expression of osteogenic marker genes compared to DMSO-treated control cells (Yeh et al., 2014). However, the authors did not provide information concerning the solvent they use for PA treatment of the cells (Yeh et al., 2014).

3.1.2. Cell-matrix and cell-cell-communication

Cell interaction between neighbouring cells, as well as communication between cells and the extracellular matrix (ECM), is mediated by different integrins (Di Benedetto et al., 2015; Schwab et al., 2013). In general, a combination of the integrin subunits α5 and β1 determines

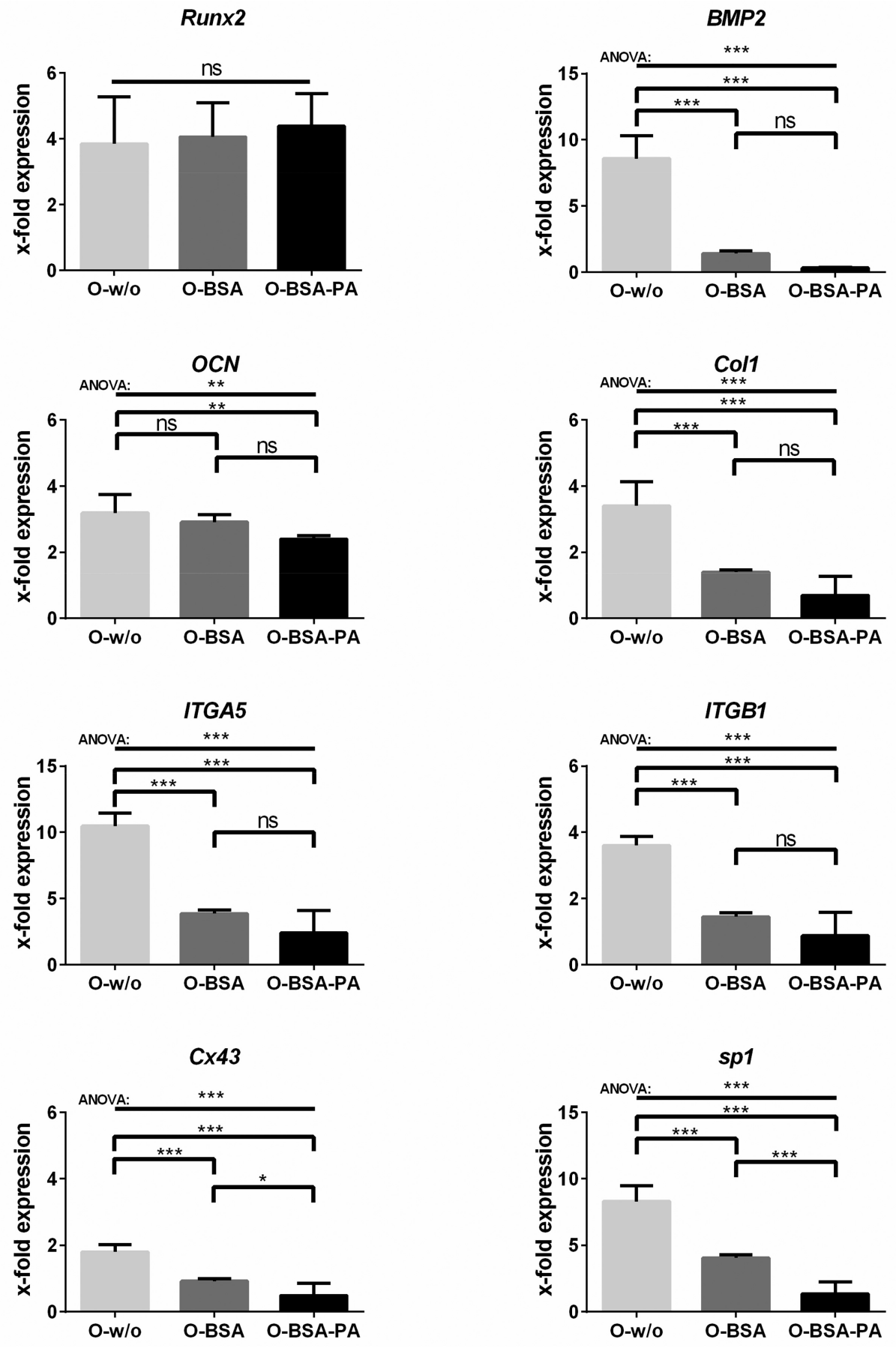

(caption on next page)

Fig. 2. Relative gene expressions of *Runx2*, *BMP2*, *OCN*, *Col1*, *ITGA5*, *ITGB1*, *Cx43*, and *sp1*. Gene expressions in osteogenic differentiated hMSCs (21 day cultivation period in all treatments) were normalized to the basal control hMSCs with corresponding supplements for representation of the x-fold change in gene expression (ΔΔCq). rt-qPCR was performed with four replicates per medium in triplets. Data is presented as mean ± SD. $*p < 0.05$, $**p < 0.01$, $***p < 0.001$.

cellular adhesion strength of cells (Roca-Cusachs et al., 2009), while expression of the integrin β1 subunit is particularly important for MSCs (Ogura et al., 2004) as its increase induces osteogenic differentiation (Di Benedetto et al., 2015). Additionally, during osteogenic differentiation of dental bud stem cells (DBSC), the expression of ITGA5 is increased and integrin β1 protein can be detected in high concentrations (Di Benedetto et al., 2015). Furthermore, during osteogenic differentiation of hBMSCs expression of integrin α5 is 4.6-fold the level of undifferentiated controls (Granéli et al., 2014).

In order to investigate the impact of BSA and PA on the expression patterns of the integrin subunits α5 and β1 (*ITGA5* and *ITGB1*) during osteogenic differentiation, we analysed the corresponding gene expression. Analysis of gene expression patterns of osteogenic markers (*Runx2*, *BMP2*, *OCN* and *Col1*) showed that *ITGA5* and *ITGB1* simultaneously increased during osteogenic differentiation of hMSCs when cultured in the medium without supplements (O-w/o), in comparison to the corresponding cells cultivated in the basal medium (*ITGA5* 10.4-fold-change; *ITGB1* 3.6-fold-change, Fig. 2). The supplementation of BSA during osteogenic differentiation induced a significant reduction in *ITGA5*, as well as *ITGB1* levels, and no substantial difference of these expression levels was observed due to the additional supplementation of PA to the medium (Fig. 2). According to this data, it can be concluded, that the cells were prevented from differentiating in the osteogenic lineage when they were exposed to BSA, as well as to BSA-PA. It is possible that reduced integrin-expression, due to the presence of BSA in the medium (Fig. 2), may have led to a reduction of the adhesion capability of the cells. It has been reported that adhesion strength is also influenced by BMP-2 as high BMP2-protein levels significantly improve the adhesion ability of primary rat BMSCs (Sun et al., 2015).

In light of the results recorded by Sun et al. (2015), it may be supposed that adhesion strength of the cells is markedly affected by both the low *integrin α5β1* and the low *BMP2* RNA levels (Fig. 2).

Integrin α5 and β1 interact with connexin 43 (cx43) (Batra et al., 2012). Cx43 is of great importance for bone homoeostasis and it mediates gap junction-facilitated communication between bone cells, as well as communication between bone cells and their microenvironment by means of hemichannels (for a review see (Plotkin and Bellido, 2013)). Cx43 is of vital relevance for osteoblastic functioning and matrix production (Stains and Civitelli, 2016). Interaction between integrin α5β1 and cx43 is mediated by C-termini of the proteins and the interaction is important for the gating mechanism of the hemichannels in response to stress (Batra et al., 2012). Cx43 expression is regulated by transcription factor sp1 (Plotkin and Bellido, 2013; Stains and Civitelli, 2016), which is mainly involved in the expression of the osteoblast genes *OCN* and *Col1* (Plotkin and Bellido, 2013).

In the present study, the osteogenic differentiation medium without supplements (O-w/o) induced a 1.8-fold increase in expression of the *cx43* gene and a 8.3-fold increase in the *sp1* gene in comparison to the corresponding basal control cells (Fig. 2). However, the long-term BSA-treatment induced a highly significant reduction in *cx43* as well as *sp1* expression, which was significantly strengthened by PA and this was in contrast to all other markers (Fig. 2).

Cx43 regulates gene expression of osteoblasts by modulating DNA binding affinity of sp1 via the extracellular signal-regulated kinase (ERK) pathway (Plotkin and Bellido, 2013; Stains and Civitelli, 2016). The activation of sp1 is regulated by signals passing through cx43 hemichannels and gap junctions (Stains and Civitelli, 2005). Following its activation, sp1 binds to connexin-response elements (CxRE) located in the proximal promotor of osteoblast genes such as collagen I (Stains and Civitelli, 2005). In hMSCs BSA administration lowered the expression levels of *Cx43* and *sp1*, as well as the levels of *BMP2* and *Col1* (Fig. 2). It can be assumed that low values of *Cx43* expression, observed in the course of BSA treatment of the cultures, caused alterations in the level of the connexin-mediated transfer and -exchange of ions. Therefore, the results of *cx43* and *sp1* gene expression, in the course of BSA-treatment of the cultures, suggested significantly reduced cell-cell-communication and cell-matrix-communication of hMSCs. This, in turn, may have led to the significant suppression of the osteogenic differentiation capability of the cells in the course of long-term treatment with supplementation of 0.045 mM BSA.

3.2. Metabolic conversion rates

In hMSCs, supplementation of 0.045 mM BSA throughout the 21-day osteogenic differentiation process induced a significant decrease in the percentage rates of glucose consumption (9.5%), pyruvate consumption (18.5%) and serine consumption (61.5%), while glutamine consumption increased significantly (17.4%) when compared to osteogenic differentiated hMSCs cultivated simultaneously in the absence of BSA ((O-w/o) control) (Fig. 3 and Table 1). Lactate and glutamate production rates were not impaired by BSA (Figs. 3 and 4). Combined, these results suggest an increase in mitochondrial glutaminolysis, as well as an impairment of the conversion of glucose and serine to lactate (Fig. 3). A shift from a glycolytic metabolic phenotype, with high conversion rates of glucose to lactate towards glucose oxidation and mitochondrial energy regeneration, is characteristic during osteogenic differentiation of stem cells (Chen et al., 2008; Pattappa et al., 2011).

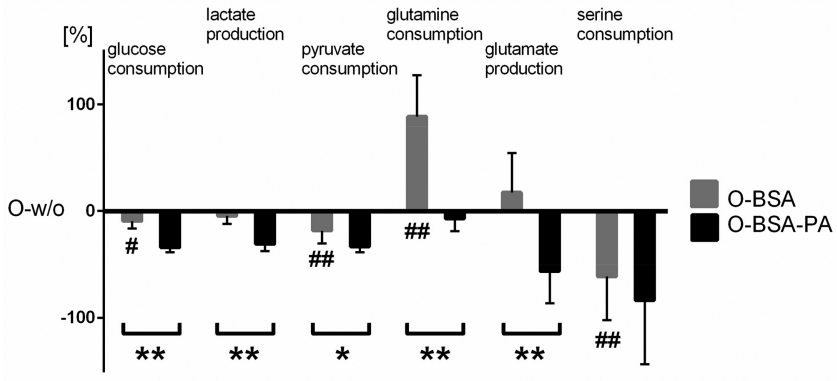

Fig. 3. The percentage changes in glucose, lactate, pyruvate, glutamine, glutamate and serine conversion rates in osteogenic differentiated hMSCs, with supplementation of 0.045 mM BSA alone (O-BSA, bars in light grey) and 0.045 mM BSA plus 0.2 mM PA (O-BSA-PA, black bars), respectively in comparison to osteogenic differentiated hMSCs without supplementation of BSA and PA (O-w/o). Positive percentage values reflect an increase of the corresponding metabolite in the BSA alone and BSA-PA group in comparison to the control group (O-w/o). Accordingly, negative percentage values reflect a decrease in the corresponding mean metabolite conversion rates. The metabolic conversion rates were measured in six wells per medium. Data is presented as mean ± SD. $\#p < 0.05$; $\#\#p < 0.01$ when the BSA alone group (O-BSA) was compared to the control group without supplementation of either BSA or BSA-PA (O-w/o). $*p < 0.05$; $**p < 0.01$ for O-BSA-PA versus O-BSA group.

Table 1
Conversion rates of glucose, lactate, pyruvate, glutamine, glutamate, and serine in osteogenic differentiated hMSCs (O-w/o), and with supplementation of 0.045 mM BSA alone (O-BSA) and 0.045 mM BSA plus 0.2 mM PA (O-BSA-PA). The metabolic conversion rates were measured in six wells per medium. All values are indicated as $x^- \pm$ SD in [nmol/(h·mg protein)]. $\#p < 0.05$; $\#\#p < 0.01$ when the BSA alone group (O-BSA) was compared to the control group without supplementation of either BSA or BSA-PA (O-w/o). $*p < 0.05$; $**p < 0.01$ for O-BSA-PA versus O-BSA group.

	O-w/o	O-BSA	O-BSA-PA
Glucose consumption	463 ± 21	419 ± 33$^{\#}$	304 ± 20**
Lactate production	505 ± 33	481 ± 38	348 ± 23**
Pyruvate consumption	54 ± 5	44 ± 7$^{\#\#}$	36 ± 2*
Glutamine consumption	70 ± 0.018	132 ± 51$^{\#\#}$	65 ± 8**
Glutamate production	23 ± 3	27 ± 10	10 ± 3**
Serine consumption	122 ± 23	32 ± 50$^{\#\#}$	20 ± 20

However, since the BSA-induced decrease in *BMP2*, *Col1*, *ITGA5* and *ITGB1* expression (Fig. 2) has indicated an attenuated osteogenic differentiation, the observed shift from glycolytic to mitochondrial energy production was probably more of a differentiation-independent effect of BSA. In porcine vascular smooth muscle strips, short-term incubation with 3% (w/v) albumin for 180 min stimulates glucose oxidation and oxygen consumption (Barron et al., 2000). Different genes of glucose transporters and glycolytic enzymes including glucose transporter 1 and 2, glucose 6-P isomerase, aldolase A and C, phosphoglycerate kinase 1 and 2, enolase, and pyruvate kinase M2 have been shown to contain sp1 binding sites in their promoters (Archer, 2011). In BSA-treated hMSCs, *sp1* expression itself, as well as the expression of *cx43*, which reduced DNA binding of sp1 to the promoters of *Runx2*, *OCN* and *Col1* were decreased (Figs. 1 and 2). Therefore, it is conceivable that the reduced glucose consumption rates observed in BSA-treated hMSCs (Fig. 3) resulted from reduced sp1 controlled expression of certain glycolytic enzymes and/or glucose transporters. In pancreatic ductal adenocarcinoma cells, the involvement of Cx43 in lactate discharging between adjacent cells is proposed (Dovmark et al., 2017). However, in the BSA-treated hMSCs, lactate release was not impaired (Fig. 3). A possible source of the unchanged rate of lactate production is glutamine. Accordingly, glutamine consumption rates increased in BSA-treated hMSCs. An interesting potential regulator of the observed BSA effects could be the mammalian target of rapamycin, which existes associated in a complex with Raptor (mTORC1) or associated with the Rictor (mTORC2). In the porcine proximal tubule cell line LLC-PK1 extracellular albumin activated mTORC1 (Peruchetti et al., 2014). In mouse embryo fibroblasts mTORC1 is shown to activate glutamine uptake (Csibi et al., 2013), which was also found in the BSA-treated hMSCs (Fig. 3). Regarding osteogenic differentiation in mouse mesenchymal stem cells loss of Raptor (which corresponds to an inhibition of mTORC1) induces a strong increase in proteins involved in osteoblast differentiation such as Runx2 and BMP2 (Martin et al., 2015). It appears that in cells from the apical papilla, suppression of the Akt-mTOR pathway enhances osteogenic differentiation (Tanaka et al., 2018). In future studies, it could be of interest to investigate whether the albumin-induced attenuation of osteogenic differentiation in our hMSCs model is associated with activation of mTORC1.

Compared to the O-BSA group, the additional supplementation of palmitate significantly decreased the conversion rates of glucose, lactate, pyruvate, glutamine and glutamate. Only serine consumption was not significantly impaired in the O-BSA-PA group, in comparison to the O-BSA group (Fig. 3). The reduction of glucose and pyruvate

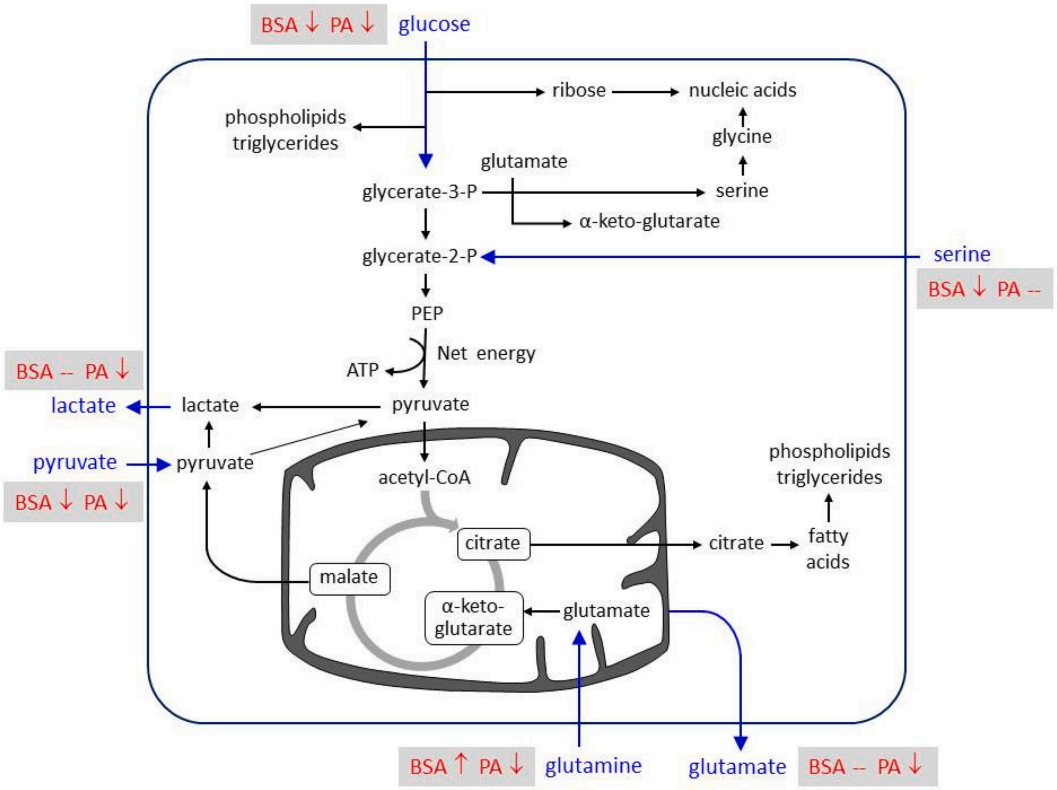

Fig. 4. Proposed model for the impact of BSA and PA on metabolic conversion rates of hMSCs after 21 days osteogenic differentiation. The blue arrows illustrate the conversion rates measured. In comparison to the untreated control, hMSC with submission of BSA alone showed a significant reduction of glucose, pyruvate and serine consumption, as well as a significant increase in glutamine consumption when compared to hMSCs osteogenic differentiated without BSA and PA. Lactate und glutamate production were not impaired by BSA. Additional supplementation of PA was accompanied by a decrease in glucose, pyruvate and glutamine consumption, as well as a decrease in lactate and glutamate production when compared to the BSA alone group.

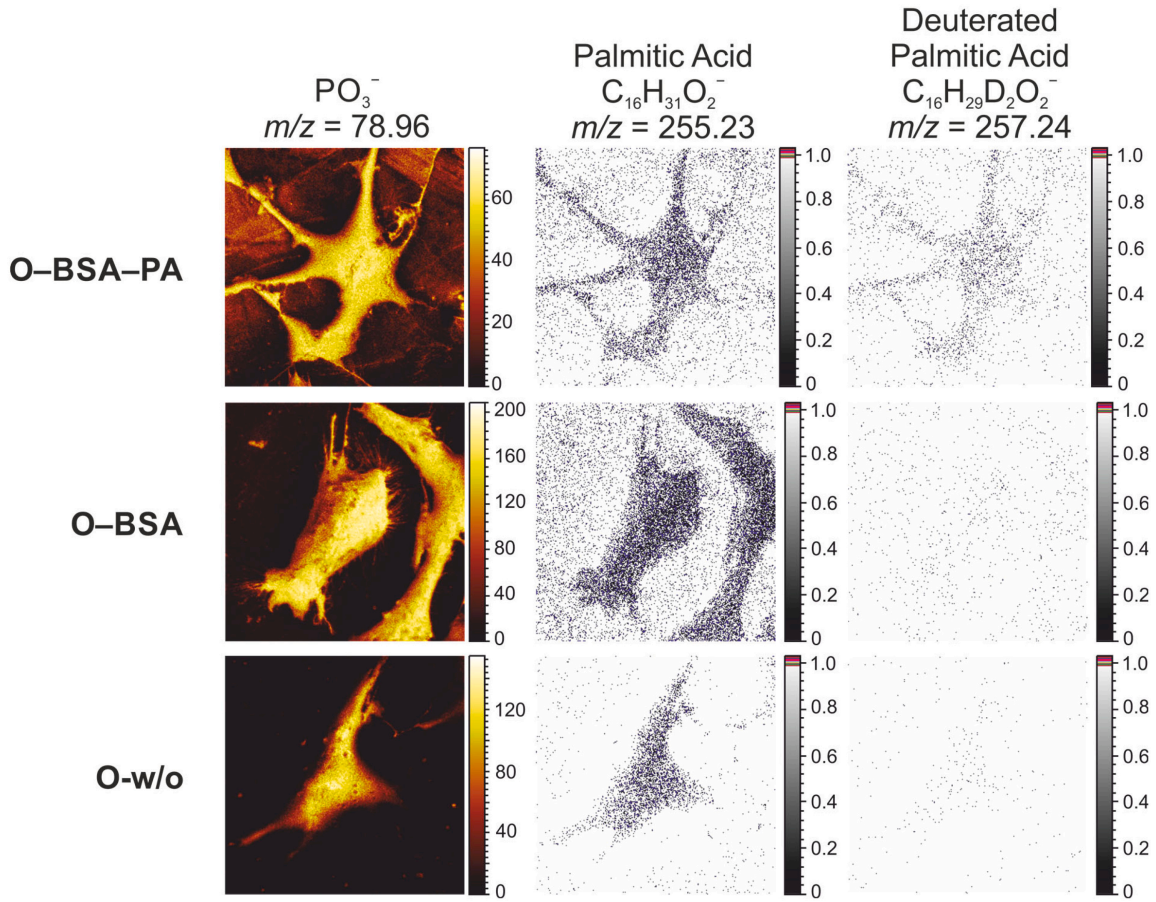

Fig. 5. ToF-SIMS secondary ion images acquired in fast imaging delayed extraction mode of an area of 150 × 150 μm^2. Images of the following signals are shown: *m/z* 78.96 – PO_3^- as a signal of phosphate groups from fragmentation of phospholipids present in the plasma membrane of cells, *m/z* 255.23 – $C_{16}H_{31}O_2^-$ – palmitate and *m/z* 257.24 – $C_{16}H_{29}D_2O_2^-$ – deuterated palmitate. All palmitate and deuterated palmitate images are binned to 3 pixels and scaled to a common colour scale to enable direct semi-quantitative comparison of the images. PO_3^- images have individual colour scales.

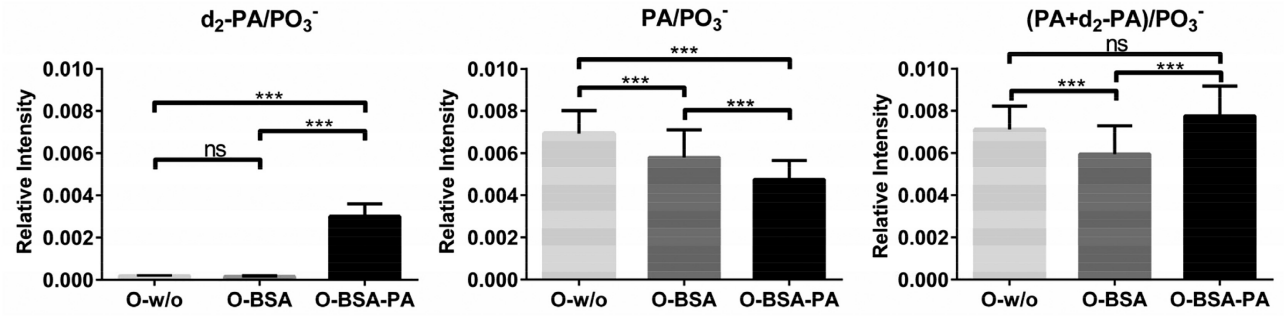

Fig. 6. Peak area plots of the relevant palmitate signals obtained by ToF-SIMS measurements in spectrometry mode. Relative intensities normalized to the PO_3^- signal are presented for the peaks at a) *m/z* 257.24 – $C_{16}H_{29}D_2O_2^-$ – deuterated palmitate (2,2-d_2-FA (16:0)), b) *m/z* 255.23 – $C_{16}H_{31}O_2^-$ – palmitate (FA(16:0), and c) for the sum of the signals of deuterated and non-deuterated palmitate. Depicted is the mean ± SEM of $n = 4$ wells per medium (with 11 measurements per well). ***$p < 0.001$.

consumption, as well as lactate production, indicates further inhibition of glycolysis by PA. The impairment of glycolysis in palmitate-treated osteogenic differentiated hMSCs may stem from the inhibition of hexokinase, the first enzyme within the glycolytic sequence by an intracellular increase in palmitate (Stewart and Blakely, 2000). The 24–48 hour treatment of undifferentiated bone marrow derived MSCs (BMMSCs), using 0.55 mM albumin and 0.4 mM palmitate, results in an inhibition of cell proliferation and induction of apoptosis, which are both prevented when the palmitate is supplemented to the medium in combination with 0.4 mM unsaturated oleic acid (Fillmore et al., 2015). In the PA + albumin treated BMMSC, glycolysis and glucose oxidation of the cells is not impaired when compared to the albumin group (Fillmore et al., 2015). The authors suggest that minimizing circulating unsaturated fatty acids could improve the clinical use of stem cells in regenerative medicine.

In hepatocellular carcinoma cells (HCC), palmitate incubation decreases the fluidity of the cell membranes which correlates with reduced glucose uptake and lactate release in a concentration-dependent manner (0–200 μM palmitate) (Lin et al., 2017). The limited glucose metabolism in palmitate treated HCC is accompanied by a decrease in the ATP: ADP ratio, which regulates AMP-dependent kinase (AMPK) activity. Lipidomic analysis of a series of HCC disclose that a decreased

content of C16:0 containing glycerophospholipids in the membrane are positively associated with the metastatic activities of the carcinomas (Lin et al., 2017).

3.3. Palmitate content of cell membranes

In order to investigate whether long-term supplementation of hMSCs has an impact on the fatty acid composition of the membranes during the osteogenic differentiation, we measured the palmitate content of the cell membranes using the surface-sensitive ToF-SIMS technique.

The palmitate supplementation was controlled with help of the surface-sensitive ToF-SIMS technique. ToF-SIMS secondary ion images illustrate the local distribution of a specific ion signal with a characteristic mass-to-charge value (m/z) by depicting its intensity in every pixel of an image. A colour scale converts this information into false-colour-images that are referred to as secondary ion images. Such secondary ion images of an exemplary cell of each group, acquired in fast imaging mode, combined with delayed extraction for high lateral resolution, are provided in Fig. 5. The PO_3^- signal results from all kinds of molecules with phosphate groups, i.e. from fragmentation of phospholipids present in the cells' plasma membrane. Consequently, it depicts the plasma membrane very well. Palmitate (FA (16:0)) was present in the plasma membranes of all groups. The deuterated palmitate (2,2-d_2-FA (16:0)) was also localized in the membrane region, but had significantly higher intensities in the group that was supplemented (O-BSA-PA) when compared to the groups without palmitate (O-BSA and O-w/o).

In spectrometry mode (high-current bunched mode), we additionally examined the relative intensity changes of the (deuterated) palmitate signals in order to expand the statistics over the analysis of a few single cells from each group. The results presented in Fig. 6 show a significant change in the relative deuterated palmitate signal intensities after supplementation (O-BSA-PA), compared to the control groups (O-BSA and O-w/o). In the control groups, relative signal intensities remained in the noise level. Deuterated palmitate (d_2-PA) supplementation decreased the cells' probability for incorporation of a non-deuterated palmitate (PA), as the PA concentration remained unchanged and both molecules were chemically equal to the cell. Hence, the cells supplemented with deuterated palmitate integrated less natural, non-deuterated palmitate into their membranes, leading to an overall unchanged level of palmitate (sum of d_2-PA and PA) in the plasma membrane.

Overall, the results suggest that the supplementation with deuterated palmitate was successful and the cells visibly integrated this additional fatty acid into their plasma membranes, while the membrane remained intact and the overall palmitate concentration (sum of deuterated and non-deuterated) remained unchanged.

4. Conclusions

Beginning with the intention to investigate the impact of palmitate on osteogenic differentiation capacity of hMSCs, we used osteogenic (OM) and basal medium (BM) in different approaches: media without supplements, and media supplemented with 0.2 mM palmitate. For this approach, the palmitate needed to be dissolved in BSA. Therefore, OM as well as BM supplemented with 0.045 mM BSA were used as controls.

After incubating hMSCs in the three different osteogenic media for 21 days, the osteogenic marker gene expression was higher than in the basal controls. Remarkably, the osteogenic medium supplemented with 0.045 mM BSA induced a significant decrease in these genes, thereby indicating a BSA-mediated attenuation of osteogenic differentiation. The additional supplementation of 0.2 mM palmitate slightly reinforced the BSA effects. The decrease of osteogenic gene expression was found to be correlated with a significant reduction of glucose and pyruvate consumption. In contrast to the attenuation of glycolysis, glutamine consumption significantly increased in these BSA-treated hMSCs. The PA significantly reinforced the BSA effect on glycolysis, but reversed the BSA effect on glutaminolysis. This was shown by a further decrease in glucose consumption and pyruvate consumption, a reduction in lactate production, as well as a decrease in glutamine consumption and glutamate production. The investigation of the fatty acid content of the hMSCs membranes, by means of *time-of-flight secondary ion mass spectrometry* (*ToF-SIMS*), revealed an increased incorporation of supplemented deuterated PA into the cell membranes, while an ultimately unchanged level of palmitate (sum of d_2-PA and PA) was evident in the plasma membrane of the cells cultivated in the three different media. Based upon this result, it can be concluded that the observed PA effects on osteogenesis and metabolism is provoked by inter- and intracellular mediated effects of palmitate.

CRediT authorship contribution statement

Kristina Glenske: Conceptualization, Investigation, Methodology, Writing - original draft. **Kaija Schäpe:** Conceptualization, Investigation, Methodology, Writing - original draft. **Anneke Wieck:** Investigation, Methodology. **Klaus Failing:** Resources. **Janina Werner:** Investigation. **Marcus Rohnke:** Conceptualization, Supervision. **Sabine Wenisch:** Conceptualization, Project administration, Supervision, Writing - review & editing. **Sybille Mazurek:** Conceptualization, Project administration, Supervision, Writing - review & editing.

This publication contains part of the doctoral thesis of Anneke Wieck.

Declaration of competing interest

None.

Acknowledgments

This work was financed by the Deutsche Forschungsgemeinschaft (DFG, Collaborative Research Centre Transregio 79 – subprojects B11 and M5). Kaija Schaepe gratefully acknowledges the financial support of the Friedrich Naumann Foundation for Freedom. We would also like to thank Tobias Hollubarsch for his assistance with data collection and evaluation, Anja Henss for many helpful discussions, and Leigh-Ann Behrendt for proofreading the manuscript.

References

Abumrad, N.A., Sfeir, Z., Connelly, M.A., Coburn, C., 2000. Lipid transporters: membrane transport systems for cholesterol and fatty acids. Current Opinion in Clinical Nutrition and Metabolic Care 3 (4), 255–262.

Archer, M.C., 2011. Role of sp transcription factors in the regulation of cancer cell metabolism. Genes & Cancer 2 (7), 712–719.

Barron, J.T., Gu, L., Rodriguez, E.R., Parrillo, J.E., 2000. Effect of serum albumin on vascular smooth muscle metabolism. Biochimica et Biophysica Acta (BBA) - Bioenergetics 1459 (1), 35–48.

Batra, N., Burra, S., Siller-Jackson, A.J., Gu, S., Xia, X., Weber, G.F., et al., 2012. Mechanical stress-activated integrin α5β1 induces opening of connexin 43 hemichannels. Proc. Natl. Acad. Sci. U. S. A. 109 (9), 3359–3364.

Chen C-T, Shih Y-RV, Kuo TK, Lee OK, Wei Y-H. Coordinated changes of mitochondrial biogenesis and antioxidant enzymes during osteogenic differentiation of human mesenchymal stem cells. Stem Cells (Dayton, Ohio) 2008;26(4):960–8.

Chen, Q., Shou, P., Zheng, C., Jiang, M., Cao, G., Yang, Q., et al., 2016. Fate decision of mesenchymal stem cells: adipocytes or osteoblasts? Cell Death Differ. 23 (7), 1128–1139.

Clabaut, A., Delplace, S., Chauveau, C., Hardouin, P., Broux, O., 2010. Human osteoblasts derived from mesenchymal stem cells express adipogenic markers upon coculture with bone marrow adipocytes. Differentiation 80 (1), 40–45.

Csibi, A., Fendt, S.-M., Li, C., Poulogiannis, G., Choo, A.Y., Chapski, D.J., et al., 2013. The mTORC1 pathway stimulates glutamine metabolism and cell proliferation by repressing SIRT4. Cell 153 (4), 840–854.

Di Benedetto, A., Brunetti, G., Posa, F., Ballini, A., Grassi, F.R., Colaianni, G., et al., 2015. Osteogenic differentiation of mesenchymal stem cells from dental bud: role of integrins and cadherins. Stem Cell Res. 15 (3), 618–628.

Dovmark, T.H., Saccomano, M., Hulikova, A., Alves, F., Swietach, P., 2017. Connexin-43 channels are a pathway for discharging lactate from glycolytic pancreatic ductal adenocarcinoma cells. Oncogene 36 (32), 4538–4550.
Ducy, P., Desbois, C., Boyce, B., Pinero, G., Story, B., Dunstan, C., et al., 1996. Increased bone formation in osteocalcin-deficient mice. Nature 382 (6590), 448–452.
Elbaz, A., Wu, X., Rivas, D., Gimble, J.M., Duque, G., 2010. Inhibition of fatty acid biosynthesis prevents adipocyte lipotoxicity on human osteoblasts in vitro. J. Cell. Mol. Med. 14 (4), 982–991.
Fillmore, N., Huqi, A., Jaswal, J.S., Mori, J., Paulin, R., Haromy, A., et al., 2015. Effect of fatty acids on human bone marrow mesenchymal stem cell energy metabolism and survival. PLoS One 10 (3), e0120257.
Gersbach, C.A., Guldberg, R.E., García, A.J., 2007. In vitro and in vivo osteoblastic differentiation of BMP-2- and Runx2-engineered skeletal myoblasts. J. Cell. Biochem. 100 (5), 1324–1336.
Glenske, K., Wagner, A.-S., Hanke, T., Cavalcanti-Adam, E.A., Heinemann, S., Heinemann, C., et al., 2014. Bioactivity of xerogels as modulators of osteoclastogenesis mediated by connexin 43. Biomaterials 35 (5), 1487–1495.
Glenske, K., Schuler, G., Arnhold, S., Elashry, M.I., Wagner, A.-S., Barbeck, M., et al., 2019. Effects of testosterone and 17β-estradiol on osteogenic and adipogenic differentiation capacity of human bone-derived mesenchymal stromal cells of postmenopausal women. Bone Reports 11.
Granéli, C., Thorfve, A., Ruetschi, U., Brisby, H., Thomsen, P., Lindahl, A., et al., 2014. Novel markers of osteogenic and adipogenic differentiation of human bone marrow stromal cells identified using a quantitative proteomics approach. Stem Cell Res. 12 (1), 153–165.
Gulin, A.A., Pavlyukov, M.S., Gusev, S.A., Malakhova, Y.N., Buzin, A.I., Chvalun, S.N., et al., 2017. Applicability of TOF-SIMS for the assessment of lipid composition of cell membrane structures. Biochemistry (Moscow). Supplement Series A: Membrane and Cell Biology 11 (2), 144–150.
Gunaratnam, K., Vidal, C., Boadle, R., Thekkedam, C., Duque, G., 2013. Mechanisms of palmitate-induced cell death in human osteoblasts. Biology Open 2 (12), 1382–1389.
Gunaratnam, K., Vidal, C., Gimble, J.M., Duque, G., 2014. Mechanisms of palmitate-induced lipotoxicity in human osteoblasts. Endocrinology 155 (1), 108–116.
Hickson-Bick, D.L.M., Sparagna, G.C., Buja, L.M., McMillin, J.B., 2002. Palmitate-induced apoptosis in neonatal cardiomyocytes is not dependent on the generation of ROS. American Journal of Physiology. Heart and Circulatory Physiology 282 (2), H656–H664.
Johansson, B., 2006. ToF-SIMS imaging of lipids in cell membranes. Surf. Interface Anal. 38 (11), 1401–1412.
Katagiri, T., Takahashi, N., 2002. Regulatory mechanisms of osteoblast and osteoclast differentiation. Oral Dis. 8 (3), 147–159.
Kim, J.-E., Ahn, M.-W., Baek, S.-H., Lee, I.K., Kim, Y.-W., Kim, J.-Y., et al., 2008. AMPK activator, AICAR, inhibits palmitate-induced apoptosis in osteoblast. Bone 43 (2), 394–404.
Lin L, Ding Y, Wang Y, Wang Z, Yin X, Yan G, et al. Functional lipidomics: palmitic acid impairs hepatocellular carcinoma development by modulating membrane fluidity and glucose metabolism. Hepatology (Baltimore, Md.) 2017.
Long, F., 2011. Building strong bones: molecular regulation of the osteoblast lineage. Nature Reviews. Molecular Cell Biology 13 (1), 27–38.
Lucas, S., Clabaut, A., Ghali, O., Haren, N., Hardouin, P., Broux, O., 2013. Implication of fatty acids in the inhibitory effect of human adipocytes on osteoblastic differentiation. Bone 55 (2), 429–430.
Martin SK, Fitter S, Dutta AK, Matthews MP, Walkley CR, Hall MN, et al. Brief report: the differential roles of mTORC1 and mTORC2 in mesenchymal stem cell differentiation. Stem Cells (Dayton, Ohio) 2015;33(4):1359–65.
Maurin, A.C., Chavassieux, P.M., Vericel, E., Meunier, P.J., 2002. Role of polyunsaturated fatty acids in the inhibitory effect of human adipocytes on osteoblastic proliferation. Bone 31 (1), 260–266.
Meunier, P., Aaron, J., Edouard, C., Vignon, G., 1971. Osteoporosis and the replacement of cell populations of the marrow by adipose tissue. A quantitative study of 84 iliac bone biopsies. Clin. Orthop. Relat. Res. 80, 147–154.
Miranda, M., Pino, A.M., Fuenzalida, K., Rosen, C.J., Seitz, G., Rodriguez, J.P., 2016. Characterization of fatty acid composition in bone marrow fluid from postmenopausal women: modification after hip fracture. J. Cell. Biochem. 117 (10), 2370–2376.
Muruganandan, S., Roman, A.A., Sinal, C.J., 2009. Adipocyte differentiation of bone marrow-derived mesenchymal stem cells: cross talk with the osteoblastogenic program. Cell. Mol. Life Sci. 66 (2), 236–253.
Ogura, N., Kawada, M., Chang, W.-J., Zhang, Q., Lee, S.-Y., Kondoh, T., et al., 2004. Differentiation of the human mesenchymal stem cells derived from bone marrow and enhancement of cell attachment by fibronectin. J. Oral Sci. 46 (4), 207–213.
Pattappa, G., Heywood, H.K., de Bruijn, J.D., Lee, D.A., 2011. The metabolism of human mesenchymal stem cells during proliferation and differentiation. J. Cell. Physiol. 226 (10), 2562–2570.
Peruchetti, D.B., Cheng, J., Caruso-Neves, C., Guggino, W.B., 2014. Mis-regulation of mammalian target of rapamycin (mTOR) complexes induced by albuminuria in proximal tubules. J. Biol. Chem. 289 (24), 16790–16801.
Pino, A.M., Rosen, C.J., Rodríguez, J.P., 2012. In osteoporosis, differentiation of mesenchymal stem cells (MSCs) improves bone marrow adipogenesis. Biol. Res. 45 (3), 279–287.
Pino, A.M., Miranda, M., Figueroa, C., Rodriguez, J.P., Rosen, C.J., 2016. Qualitative aspects of bone marrow adiposity in osteoporosis. Front. Endocrinol. 7, 139.
Plotkin, L.I., Bellido, T., 2013. Beyond gap junctions: Connexin43 and bone cell signaling. Bone 52 (1), 157–166.
Polak-Jonkisz, D., Zwolinska, D., 1998. Osteocalcin as a biochemical marker of bone turnover. Nephrology 4, 339–346.
Roca-Cusachs, P., Gauthier, N.C., Del Rio, A., Sheetz, M.P., 2009. Clustering of alpha(5) beta(1) integrins determines adhesion strength whereas alpha(v)beta(3) and talin enable mechanotransduction. Proc. Natl. Acad. Sci. U. S. A. 106 (38), 16245–16250.
Schaepe, K., Kokesch-Himmelreich, J., Rohnke, M., Wagner, A.-S., Schaaf, T., Wenisch, S., et al., 2015. Assessment of different sample preparation routes for mass spectrometric monitoring and imaging of lipids in bone cells via ToF-SIMS. Biointerphases 10 (1), 19016.
Schaepe K, Kokesch-Himmelreich J, Rohnke M, Wagner A-S, Schaaf T, Henss A, et al. Storage of cell samples for ToF-SIMS experiments—How to maintain sample integrity. Biointerphases 2016;11(2):02A313.
Schaepe, K., Werner, J., Glenske, K., Bartges, T., Henss, A., Rohnke, M., et al., 2017. ToF-SIMS study of differentiation of human bone-derived stromal cells: new insights into osteoporosis. Anal. Bioanal. Chem. 409 (18), 4425–4435.
Schwab, E.H., Halbig, M., Glenske, K., Wagner, A.-S., Wenisch, S., Cavalcanti-Adam, E.A., 2013. Distinct effects of RGD-glycoproteins on integrin-mediated adhesion and osteogenic differentiation of human mesenchymal stem cells. Int. J. Med. Sci. 10 (13), 1846–1859.
Singh, L., Brennan, T.A., Russell, E., Kim, J.-H., Chen, Q., Brad Johnson, F., et al., 2016. Aging alters bone-fat reciprocity by shifting in vivo mesenchymal precursor cell fate towards an adipogenic lineage. Bone 85, 29–36.
Stains, J.P., Civitelli, R., 2005. Cell-to-cell interactions in bone. Biochem. Biophys. Res. Commun. 328 (3), 721–727.
Stains, J.P., Civitelli, R., 2016. Connexins in the skeleton. Semin. Cell Dev. Biol. 50, 31–39.
Stewart, J.M., Blakely, J.A., 2000. Long chain fatty acids inhibit and medium chain fatty acids activate mammalian cardiac hexokinase. Biochim. Biophys. Acta 1484 (2–3), 278–286.
Sun, J., Li, J., Li, C., Yu, Y., 2015. Role of bone morphogenetic protein-2 in osteogenic differentiation of mesenchymal stem cells. Mol. Med. Rep. 12 (3), 4230–4237.
Tanaka, Y., Sonoda, S., Yamaza, H., Murata, S., Nishida, K., Hama, S., et al., 2018. Suppression of AKT-mTOR signal pathway enhances osteogenic/dentinogenic capacity of stem cells from apical papilla. Stem Cell Res Ther 9 (1), 334.
Trigatti, B.L., Gerber, G.E., 1995. A direct role for serum albumin in the cellular uptake of long-chain fatty acids. Biochem. J. 308 (1), 155–159.
Unterluggauer, H., Mazurek, S., Lener, B., Hutter, E., Eigenbrodt, E., Zwerschke, W., et al., 2008. Premature senescence of human endothelial cells induced by inhibition of glutaminase. Biogerontology 9 (4), 247–259.
Vanbellingen, Q.P., Elie, N., Eller, M.J., Della-Negra, S., Touboul, D., Brunelle, A., 2015. Time-of-flight secondary ion mass spectrometry imaging of biological samples with delayed extraction for high mass and high spatial resolutions. Rapid Communications in Mass Spectrometry RCM 29 (13), 1187–1195.
Verma, S., 2002. Adipocytic proportion of bone marrow is inversely related to bone formation in osteoporosis. J. Clin. Pathol. 55 (9), 693–698.
Vimalraj, S., Arumugam, B., Miranda, P.J., Selvamurugan, N., 2015. Runx2: structure, function, and phosphorylation in osteoblast differentiation. Int. J. Biol. Macromol. 78, 202–208.
Wagner A-S, Glenske K, Henß A, Kruppke B, Rößler S, Hanke T, et al. Cell behavior of human mesenchymal stromal cells in response to silica/collagen based xerogels and calcium deficient culture conditions. Biomedical Materials (Bristol, England) 2017;12(4):45003.
Wang, D., Haile, A., Jones, L.C., 2013. Dexamethasone-induced lipolysis increases the adverse effect of adipocytes on osteoblasts using cells derived from human mesenchymal stem cells. Bone 53 (2), 520–530.
Wang L, Li Z-Y, Wang Y-P, Wu Z-H, Yu B. Dynamic expression profiles of marker genes in osteogenic differentiation of human bone marrow-derived mesenchymal stem cells. Chinese Medical Sciences Journal = Chung-kuo i hsueh k'o hsueh tsa chih 2015;30(2):108–13.
Wei, J., Karsenty, G., 2015. An overview of the metabolic functions of osteocalcin. Current Osteoporosis Reports 13 (3), 180–185.
Wenisch, S., Trinkaus, K., Hild, A., Hose, D., Herde, K., Heiss, C., et al., 2005. Human reaming debris: a source of multipotent stem cells. Bone 36 (1), 74–83.
Wenisch, S., Trinkaus, K., Hild, A., Hose, D., Heiss, C., Alt, V., et al., 2006. Immunochemical, ultrastructural and electrophysiological investigations of bone-derived stem cells in the course of neuronal differentiation. Bone 38 (6), 911–921.
Wu, L., Feyerabend, F., Schilling, A.F., Willumeit-Römer, R., Luthringer, Bérengère, J.C., 2015. Effects of extracellular magnesium extract on the proliferation and differentiation of human osteoblasts and osteoclasts in coculture. Acta Biomater. 27, 294–304.
Yeh, L.-C.C., Ma, X., Ford, J.J., Adamo, M.L., Lee, J.C., 2013. Rapamycin inhibits BMP-7-induced osteogenic and lipogenic marker expressions in fetal rat calvarial cells. J. Cell. Biochem. 114 (8), 1760–1771.
Yeh, L.-C.C., Ford, J.J., Lee, J.C., Adamo, M.L., 2014. Palmitate attenuates osteoblast differentiation of fetal rat calvarial cells. Biochem. Biophys. Res. Commun. 450 (1), 777–781.